Light-Driven Tyrosine Radical Formation in a Ruthenium–Tyrosine Complex Attached to Nanoparticle TiO$_2$

Raed Ghanem,[†] Yunhua Xu,[‡] Jie Pan,[†] Tobias Hoffmann,[‡] Johan Andersson,[†] Tomáš Polívka,[†] Torbjörn Pascher,[†] Stenbjörn Styring,[§] Licheng Sun,*,[‡] and Villy Sundström*,[†]

Departments of Chemical Physics and Biochemistry, Lund University, P.O. Box 124, S-22100 Lund, Sweden, and Department of Organic Chemistry, Stockholm University, S-10691 Stockholm, Sweden

We demonstrate a possibility of multistep electron transfer in a supramolecular complex adsorbed on the surface of nanocrystalline TiO$_2$. The complex mimics the function of the tyrosine$_Z$ and chlorophyll unit P$_{680}$ in natural photosystem II (PSII). A ruthenium(II) tris(bipyridyl) complex covalently linked to a L-tyrosine ethyl ester through an amide bond was attached to the surface of nanocrystalline TiO$_2$ via carboxylic acid groups linked to the bpy ligands. Synthesis and characterization of this complex are described. Excitation (450 nm) of the complex promotes an electron to a metal-to-ligand charge-transfer (MLCT) excited state, from which the electron is injected into TiO$_2$. The photogeneration of Ru(III) is followed by an intramolecular electron transfer from tyrosine to Ru(III), regenerating the photosensitizer Ru(II) and forming the tyrosyl radical. The tyrosyl radical is formed in less than 5 μs with a yield of 15%. This rather low yield is a result of a fast back electron transfer reaction from the nanocrystalline TiO$_2$ to the photogenerated Ru(III).

Introduction

The mechanism of photosynthetic water oxidation into molecular oxygen in photosystem II (PSII) has been extensively studied.[1,2] Light is absorbed by the primary donor chlorophyll unit P$_{680}$, and then, an electron is transferred from the excited state chlorophyll, via several steps, to quinone on the acceptor side of PSII, leading to the oxidation of P$_{680}$. Photogenerated P$_{680}^+$ recaptures an electron by oxidizing a nearby tyrosine (Tyr$_Z$), located approximately 8 Å away from P$_{680}$, into a neutral tyrosyl radical (Tyr$_Z$•).[1] This radical in its turn oxidizes a tetranuclear Mn-cluster bound to PSII,

and after four consecutive turnovers, two water molecules are oxidized into molecular oxygen. Moreover, recent results proposed that the Tyr$_Z$ itself catalyzes water oxidation by abstracting a hydrogen atom from a water molecule coordinated to the manganese cluster Mn$_4$.[3] This shows that the Tyr$_Z$ plays a crucial role in this process whatever the exact mechanism of photosynthetic water oxidation is.[3]

Many efforts have been made in recent years to design and synthesize supramolecular complexes to mimic the important parts of the light-driven process in PSII in order to construct an artificial photosynthetic system for fuel production using reducing equivalents from water.[4] Because photophysical properties and electrochemical behavior of ruthenium(II) tris(bipyridyl) complexes are well studied,[5] and because they are photochemically stable and easy to functionalize with a long-lived excited state, they are suitable

* Corresponding authors. E-mail: villy.sundstrom@chemphys.lu.se (V.S.); licheng.sun@organ.su.se (L.S.). Fax: +46-46-2224119 (V.S.); fax +46-8-154908 (L.S.).
† Department of Chemical Physics, Lund University.
‡ Stockholm University.
§ Department of Biochemistry, Lund University.

 (1) (a) Tommos, C.; Tang, X. S.; Warncke, K.; Hoganson, C. W.; Styring, S.; McCracken, J.; Diner, B. A.; Babcock, G. T. *J. Am. Chem. Soc.* **1995**, *117*, 10325. (b) Hoganson, C. W.; Lydakis-Simantiris, N.; Tang, X. S.; Tommos, C.; Warncke, K.; Babcock, G. T.; Diner, B. A.; McCracken, J.; Styring, S. *Photosynth. Res.* **1995**, *46*, 177. (c) Vermaas, W.; Styring, S.; Schröder, W.; Anderson, B. *Photosynth. Res.* **1993**, *38*, 249. (d) For recent reviews on photosynthetic water oxidation, see: *Biochim. Biophys. Acta* **2001**, *1503* (1−2), 5.
 (2) Yachandra, V. K.; De Rose, V. J.; Latimer, M. J.; Mukerji, I.; Sauer, K.; Klein, M. P. *Science* **1993**, *260*, 675.
 (3) (a) Hoganson, C. W.; Babcock, G. T. *Science* **1997**, *277*, 1953. (b) Yagi, M.; Kaneko, M. *Chem. Rev.* **2001**, *101*, 21.
 (4) (a) Sun, L.; Hammarström, L.; Åkermark, B.; Styring, S. *Chem. Soc. Rev.* **2001**, *30* (1), 36. (b) Hammarström, L.; Sun, L.; Åkermark, B.; Styring, S. *Biochim. Biophys. Acta* **1998**, *1365* (1−2), 193.
 (5) (a) Kalyanasundaram, K. *Photochemistry of Polypyridine and Porphyrin Complexes*; Academic Press: London, 1992; Chapter 6. (b) Meyer, T. J. *Acc. Chem. Res.* **1989**, *22*, 163. (c) Juris, A.; Balzani, V.; Barigelletti, F.; Campagna, S.; Belser, P.; Vonzelewsky, A. *Coord. Chem. Rev.* **1988**, *84*, 85.

candidates to mimic the function of P_{680} in PSII. To achieve this goal, ruthenium(II) tris(bipyridyl) complexes were connected to L-tyrosine ethyl ester (to mimic the Tyr$_Z$) through an amide bridge.[4,6−8] In previous studies, it was shown that a model complex such as Ru(II)(bpy)$_2$(4-Me-4′-CONH-L-tyrosine ethyl ester-2,2′-bpy)·2PF$_6$ in the presence of an external electron acceptor (methyl viologen, MV^{2+}) mimics the Tyr$_Z$-P_{680} functional unit of PSII by generating a tyrosyl radical by means of intramolecular electron transfer from the tyrosine moiety to the photogenerated Ru(III).[4,6−8] It was also demonstrated that the photogenerated tyrosyl radical can oxidize a binuclear manganese cluster from its Mn(III/III) state to the Mn(III/IV) state.[7] Sjödin et al.[8] showed that protonation/deprotonation of the tyrosine moiety in this Ru−tyrosine complex strongly affects the intramolecular electron transfer reaction from tyrosine to the photogenerated Ru(III). They found that at pH below the tyrosine p$K_a \approx$ 10, where the tyrosine group is initially protonated, the rate constant increases with pH, while deprotonation of the tyrosine group (at pH >10) results in a high and pH independent rate constant. The pH and temperature dependence of the intramolecular electron transfer rate indicate that this reaction occurs as a concerted electron transfer/deprotonation reaction. The similarity in pH dependence and activation energy for the electron transfer from Tyr$_Z$ to P_{680}^+ in manganese depleted PSII suggested the same mechanism in the artificial and natural systems.[8,9]

Despite the proven functionality of the artificial system, use of an external electron acceptor such as MV^{2+} or cobalt pentaaminechloride ($[Co(NH_3)_5Cl]^{2+}$) has the disadvantage of diffusion limited electron transfer from the excited state of the ruthenium complex to the external electron acceptor.[4,6−8] It is known that, through dye molecule sensitization of a wide band gap semiconductor such as TiO₂, electrons can be injected from the excited state of the dye into the semiconductor. Recently, electron transfer between nanostructured TiO₂ and dye sensitizers has been intensively studied.[10−19] Electron injection was reported to occur on the femtosecond to picosecond time scale.[17,18] Thus, the use of a nanocrystalline TiO₂ semiconductor as an electron acceptor for the Ru−tyrosine complex will overcome the diffusion controlled

Chart 1. Complex **1** and Its Analogue Complex **1a** Synthesized as Shown in Scheme 1

1

1a
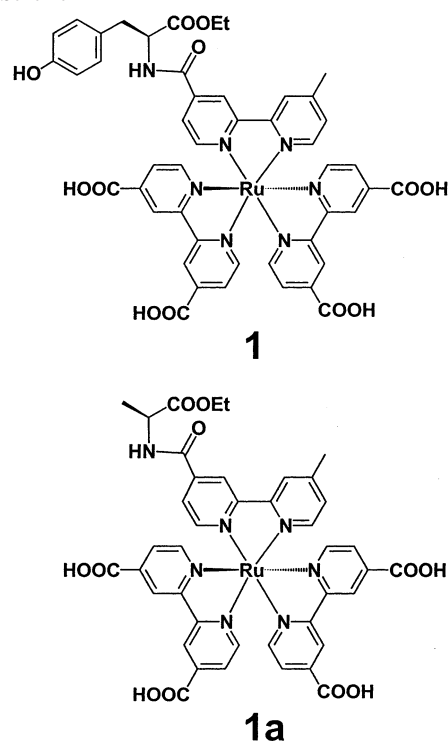
nature of the electron transfer and, therefore, will enable us to measure the true rate of the tyrosine-to-Ru(III) electron transfer step.

We have synthesized new complex **1** (Chart 1), which can be attached to nanocrystalline TiO₂ via four carboxylic acid groups attached to the bipyridine ligand. With this system (Figure 1), we will demonstrate the possibility of obtaining a multistep electron transfer in a supramolecular complex system incorporating tyrosine and a Ru(II) tris(bipyridyl) complex to mimic the function of the Tyr$_Z$ and the P_{680} in the natural PSII.

Experimental Section

Materials. 4,4′-Dimethyl-2,2′-bipyridine (Me₂bpy), RuCl₃·xH₂O, L-tyrosine ethyl ester hydrochloride, and L-alanine ethyl ester hydrochloride were purchased from Aldrich.

4-Carboxy-4′-methyl-2,2′-bipyridine (2). This compound was synthesized according a literature procedure.[20] ¹H NMR (300 MHz, DMSO-d_6), δ in ppm: 8.84 (d, $J = 5.1$ Hz, 1H, bpy-H); 8.80 (s, 1H, bpy-H); 8.56 (d, $J = 5.1$ Hz, 1H, bpy-H); 8.25 (s, 1H, bpy-H); 7.84 (m, 1H, bpy-H); 7.31 (d, $J = 5.2$ Hz, 1H, bpy-H); 2.41 (s, 3H, bpy-CH₃).

(6) Magnuson, A.; Berglund, H.; Korall, P.; Hammarström, L.; Åkermark, B.; Styring, S.; Sun, L. *J. Am. Chem. Soc.* **1997**, *119*, 10720.
(7) Magnuson, A.; Frapart, Y.; Abrahamsson, M.; Horner, O.; Berglund, H.; Korall, P.; Åkermark, B.; Styring, S.; Jean-Jacques, G.; Hammarström, L.; Sun, L. *J. Am. Chem. Soc.* **1999**, *121*, 89.
(8) Sjödin, M.; Styring, S.; Åkermark, B.; Sun, L.; Hammarström, L. *J. Am. Chem. Soc.* **2000**, *122* (16), 3932.
(9) Ahlbrink, R.; Haumann, M.; Cherepanov, D.; Bogerhausen, O.; Mulkidjanian, A.; Junge, W. *Biochemistry* **1998**, *37*, 1131.
(10) Hilgendorff, M.; Sundström, V. *J. Phys. Chem B* **1998**, *102* (51), 10505.
(11) Nazeruddin, M. K.; Muller, E.; Humphry-Baker, R.; Vlachopoulos, N.; Grätzel, M. *J. Chem. Soc., Dalton Trans.* **1997**, 4571.
(12) Thompson, A.; Smailes, M.; Jeffery, J.; Ward, M. *J. Chem. Soc., Dalton Trans.* **1997**, 737.
(13) Nazeruddin, M. K.; Zakeeruddin, S. M.; Humphry-Baker, R.; Jirousek, M.; Liska, P.; Vlachopoulos, N.; Shklover, V.; Fischer, C. H.; Grätzel, M. *Inorg. Chem.* **1999**, *38*, 6298.
(14) Chen, C.; Qi, X.; Zhou, B. *J. Photochem. Photobiol., A* **1997**, *109*, 155.
(15) Ghenne, E.; Dumont, F.; Buss-Herman, C. *Colloid Surf., A* **1998**, *131* (1−3) 63.
(16) Kamat, V. *J. Phys. Chem.* **1989**, *93*, 859.

(17) For electron injection studies on different dye-sensitized TiO₂ systems, see the recent review articles: (a) Asbury, J. B.; Hao, E.; Wang, Y.; Ghosh, H. H.; Lian, T. *J. Phys. Chem. B* **2001**, *105*, 4545. (b) Grätzel, M.; Moser, J.-E. Solar Energy Conversion. In *Electron Transfer in Chemistry*; Balzani, V., Gould, I., Eds.; Vol. V, Wiley-VCH: Weinheim, 2001; p 589.
(18) (a) Benkö, G.; Kallioinen, J.; Korppi-Tommola, J. E.; Yartsev, A. P.; Sundström, V. *J. Am. Chem. Soc.* **2002**, *124*, 489. (b) Kallioinen, J.; Benkö, G.; Sundström, V.; Korppi-Tommola, J. E. I.; Yartsev, A. P. *J. Phys. Chem. B* **2002**, *106*, 4396.
(19) Argazzi, R.; Bignozzi, C.; Heimer, T.; Castellano, F.; Meyer, G. *J. Phys. Chem. B* **1997**, *101*, 2591.
(20) McCafferty, D. G.; Bishop, B. M.; Wall, C. G.; Hughes, S. G.; Mecklenberg, S. L.; Meyer, T. J.; Erickson, B. W. *Tetrahedron* **1995**, *51*, 1093.
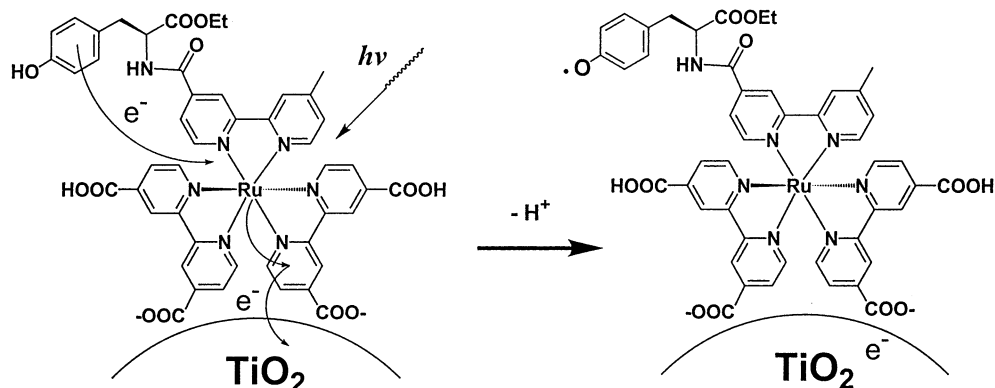
Figure 1. Reaction scheme proposed for the photoinduced electron transfer in the $1-TiO_2$ system. (I) Excitation of Ru(II)(bpy)$_3$ moiety. (II) Electron injection from the excited state of the Ru(II) complex to the TiO_2 producing Ru(III). (III) Intramolecular electron transfer from the tyrosine moiety to Ru(III) leading to recovery of the Ru(II) and tyrosyl radical formation.

4,4′-Dicarboxy-2,2′-bipyridine (4). This compound was synthesized according a literature procedure.[21] ^{1}H NMR (400 MHz, DMSO-d6), δ in ppm: 8.90 (m, 2H, bpy-H); 8.83 (s, 2H, bpy-H); 7.90 (dd, $J = 4.8$ Hz, 1.6 Hz, 2H, bpy-H).

4-Me-2,2′-bpy-4′-CONH-l-Tyrosine Ethyl Ester (3). Compound **2** (663 mg, 3.1 mmol) and thionyl chloride (30 mL) were heated to reflux for 4 h. After the excess thionyl chloride was evaporated, a white solid remained in the flask, and it was dried under vacuum at 60 °C for 2 h. The solid was dissolved in dry acetonitrile, and the obtained solution was dropped into another acetonitrile solution, which had L-tyrosine ethyl ester hydrochloride (845 mg, 3.4 mmol) and triethylamine (1.0 mL) at room temperature within 20 min. The mixture was heated to reflux for another 4 h. After the solution was cooled to room temperature, white crystals (triethylamine hydrochloride) were formed. After the crystals were filtered off, the filtrate was concentrated to near dryness, and the residue was redissolved in dichloromethane and washed three times with 0.1 M hydrochloric acid. The organic phase was dried over anhydrous sodium sulfate and evaporated to dryness, crude products were purified by column chromatography on silica gel (MeOH/CHCl$_3$ 5/95), and white crystals of **3** were obtained. ^{1}H NMR (300 MHz, CDCl$_3$), δ in ppm: 8.78 (d, $J = 5.1$ Hz, 1H, bpy-H), 8.61 (s, 1H, bpy-H), 8.55 (d, $J = 5.1$ Hz, 1H, bpy-H), 8.24 (s, 1H, bpy-H), 7.67 (dd, $J = 4.9$, 1.8 Hz, 1H, bpy-H), 7.17 (d, $J = 5.1$ Hz, 1H, bpy-H), 7.01 (d, $J = 8.4$ Hz, 2H, ph-H), 6.88 (d, $J = 6.6$ Hz, 1H, NH), 6.71 (d, $J = 8.7$ Hz, 2H, ph-H), 5.04 (m, 1H, CH(COOEt)), 4.23 (q, $J = 7.2$ Hz, 2H, COOEt), 3.20 (m, 2H, CH$_2$-ph), 2.45 (s, 3H, bpy-CH$_3$), 1.28 (t, $J = 7.2$ Hz, 3H, COOEt).

4-Me-2,2′-bpy-4′-CONH-l-Alanine Ethyl Ester (3a). The synthesis of this compound was similar to the procedure for the preparation of **3**, except that L-alanine ethyl ester hydrochloride was used as the starting material instead of L-tyrosine ethyl ester hydrochloride. ^{1}H NMR (400 MHz, CDCl$_3$), δ in ppm: 8.77 (d, $J = 4.8$ Hz, 1H, bpy-H), 8.66 (s, 1H, bpy-H), 8.53 (d, $J = 5.2$ Hz, 1H, bpy-H), 8.24 (s, 1H, bpy-H), 7.74 (dd, $J = 5.2$, 1.6 Hz, 1H, bpy-H), 7.15 (d, $J = 5.2$ Hz, 1H, bpy-H), 7.10 (d, $J = 6.8$ Hz, 1H, NH), 4.79 (m, 1H, CH(COOEt)), 4.24 (q, $J = 7.6$ Hz, 2H, COOEt), 2.44 (s, 3H, bpy-CH$_3$), 1.55 (d, $J = 6.8$ Hz, 3H, CH(COOEt)CH$_3$), 1.30 (t, $J = 7.2$ Hz, 3H, COOEt).

4,4′-Di-COOEt-2,2′-bpy (5). This compound was synthesized according a literature procedure (ref 22).^{1}H NMR (300 MHz, CDCl$_3$), δ in ppm: 8.94 (s, 2H, bpy-H); 8.86 (d, $J = 4.8$ Hz, 2H,

bpy-H); 7.91 (d, $J = 4.8$ Hz, 2H, bpy-H); 4.46 (q, $J = 7.2$ Hz, 4H, COOEt); 1.45 (t, $J = 7.2$ Hz, 6H, COOEt).

***cis*-Ru(4,4′-di-COOEt-2,2′-bpy)$_2$Cl$_2$ (6).** This complex was synthesized according a modification of a literature procedure (ref 22). The purification of the final product was conducted by column chromatography on silica gel (eluents: ethanol and dichloromethane, 20/80, v/v). ^{1}H NMR (400 MHz, DMSO-d$_6$), δ in ppm: 10.09 (d, $J = 6.0$ Hz, 1H, bpy-H); 9.11 (s, 1H, bpy-H); 8.92 (s, 1H, bpy-H); 8.24 (dd, $J = 6.0$ Hz, 1.6 Hz, 1H, bpy-H); 7.74 (d, $J = 5.6$ Hz, 1H, bpy-H); 7.47 (dd, $J = 6.0$ Hz, 1.6 Hz, 1H, bpy-H); 4.51 (q, $J = 6.8$ Hz, 2H, COOEt); 4.34 (q, $J = 7.2$ Hz, 2H, COOEt); 1.43 (t, $J = 6.8$ Hz, 3H, COOEt); 1.29 (t, $J = 7.2$ Hz, 3H, COOEt).

Ru(II)(4,4′-di-COOEt-2,2′-bpy)$_2$(4-Me-2,2′-bpy-4′-CONH-l-tyrosine Ethyl Ester)(PF$_6$)$_2$ (7). Compounds **3** (83 mg, 0.2 mmol) and **6** (155 mg, 0.2 mmol) were mixed in methanol (20 mL) and water (10 mL). The mixture was heated to reflux for 8 h in N$_2$ atmosphere, and strong light was avoided. An orange-brown solution was obtained. After the solvent was removed under reduced pressure, the crude product was purified by column chromatography on silica gel (eluent CH$_3$CN/H$_2$O/saturated aqueous KNO$_3$, 10/3/1, v/v/v). Excess KNO$_3$ was removed from the product by evaporating CH$_3$CN and most of H$_2$O under reduced pressure and then adding acetonitrile to precipitate KNO$_3$. After filtering off the KNO$_3$ precipitate, the solvent was removed under reduced pressure, leaving the product as the nitrate salt, which was redissolved in water and precipitated with a concentrated solution of ammonium hexafluorophosphate. The precipitate was filtered, washed with water and then ether, and dried in a vacuum to afford **7** as PF$_6^-$ salt. ^{1}H NMR (300 MHz, CD$_3$CN), δ in ppm: 9.07 (s, 4H, 4,4′-di-COOEt-bpy-H), 8.72 (s, 1H, 4′-Me-bpy-H), 8.52 (s, 1H, 4′-Me-bpy-H), 7.77−7.97 (m, 9H, 4,4′-di-COOEt-bpy-H (8H)+4′-Me-bpy-H (1H)), 7.56−7.62 (m, 2H, 4′-Me-bpy-H + ph-OH), 7.50 (d, $J = 5.7$ Hz, 1H, 4′-Me-bpy-H), 7.31 (d, $J = 6.4$ Hz, 1H, 4′-Me-bpy-H), 7.11 (m, 2H, ph-H), 6.86 (d, $J = 6.4$ Hz, 1H, NH), 6.73 (m, 2H, ph-H), 4.82 (m, 1H, CH(COOEt)), 4.49 (m, 8H, 4,4′-di-COOCH$_2$CH$_3$-bpy), 4.17 (m, 2H, CH(COOCH$_2$CH$_3$)), 3.03−3.25 (m, 2H, CH$_2$-ph), 2.59 (s, 3H, bpy-CH$_3$), 1.43 (m, 12H, 4,4′-di-COOCH$_2$CH$_3$-bpy), 1.23 (m, 3H, CH(COOCH$_2$CH$_3$)). The electrospray ionization mass spectrometry (ESI-MS) spectrum of **7** from acetonitrile gave a monocharged peak at m/z 1252.2 (calculated for [M − PF$_6^-$]$^+$, 1252.2) and a doubly charged peak at m/z 553.6 (calculated for [M − 2PF$_6^-$]$^{2+}$, 553.6).

Ru(II)(4,4′-di-COOEt-2,2′-bpy)$_2$(4-Me-2,2′-bpy-4′-CONH-l-alanine Ethyl Ester)(PF$_6$)$_2$ (7a). The synthesis of this compound was similar to that for **7**, except that **3a** was used instead of **3**. ^{1}H

(21) Sprintschnik, G.; Sprintschnik, H. W.; Kirsch, P. P.; Whitten, D. G. *J. Am. Chem. Soc.* **1977**, *99*, 4947.

(22) Kormann, C.; Bahnemann, W.; Hoffmann, R. *J. Phys. Chem.* **1988**, *92*, 5196.

NMR (300 MHz, CD₃CN), δ in ppm: 9.07 (s, 4H, 4,4′-di-COOEt-bpy-H), 8.82 (s, 1H, 4′-Me-bpy-H), 8.57 (s, 1H, 4′-Me-bpy-H), 7.98 (d, J = 6.0 Hz, 1H, 4′-Me-bpy-H), 7.82−7.99 (m, 8H, 4,4′-di-COOEt-bpy-H), 7.71 (dd, J = 6.0 Hz,1.5 Hz, 1H, 4′-Me-bpy-H), 7.67 (d, J = 6.9 Hz, 1H, 4′-Me-bpy-H), 7.52 (d, J = 6.0 Hz, 1H, 4′-Me-bpy-H), 7.22 (d, J = 5.7 Hz, 1H, NH), 4.61 (m, 1H, CH-(COOEt)), 4.49 (q + q, J = 7.2 Hz, 8H, 4,4′-di-COOCH₂CH₃-bpy), 4.18 (q, J = 6.9 Hz, 2H, CH(COOCH₂CH₃)), 2.59 (s, 3H, bpy-CH₃), 1.52 (d, J = 7.2 Hz, 3H, CH(COOEt)-CH₃), 1.44 (t + t, J = 7.2 Hz, 12H, 4,4′-di-COOCH₂CH₃-bpy), 1.26 (t, J = 7.2 Hz, 3H, CH(COOCH₂CH₃)). ESI-MS spectrum of **7a** from acetonitrile gave a monocharged peak at m/z 1160.2 (calculated for [M − PF₆⁻]⁺, 1160.2) and a doubly charged peak at m/z 507.6 (calculated for [M − 2PF₆⁻]²⁺, 507.6).

Ru(II)(4,4′-di-COOH-2,2′-bpy)₂(4-Me-2,2′-bpy-4′-CONH-l-tyrosine Ethyl Ester)(PF₆)₂ (1). A solution of **7** (140 mg, 0.1 mmol) in acetone (10 mL) and 4 M NaOH (0.1 mL, 0.4 mmol) was refluxed under N₂ and in the dark for 4 h. After the solution was cooled to room temperature, orange precipitate appeared, and it was filtered and washed with acetone. The solid was redissolved in water (7 mL), and a few drops of 2 M HCl aqueous solution were added. The obtained precipitate again was filtered off, washed with water, and then dried under vacuum. ¹H NMR (300 MHz, D₂O + NaOH), δ in ppm: 8.73 (s, 4H, 4,4′-di-COOH-bpy-H), 8.52 (s, 1H, 4′-Me-bpy-H), 8.29 (s, 1H, 4′-Me-bpy-H), 7.69−7.76 (m, 5H, 4,4′-di-COOH-bpy-H (4H) + 4′-Me-bpy-H (1H)), 7.53−7.55 (m, 4H, 4,4′-di-COOH-bpy-H), 7.43 (d, J = 5.6 Hz, 1H, 4′-Me-bpy-H), 7.37 (m, 1H, 4′-Me-bpy-H), 7.12 (d, J = 5.6 Hz, 1H, 4′-Me-bpy-H), 6.88 (d, J = 8.4 Hz, 2H, ph-H), 6.40 (d, J = 8.4 Hz, 2H, ph-H), 4.48 (m, 1H, CH(COOEt)), 3.50 (q, J = 6.8 Hz, 2H, COOCH₂CH₃), 2.74−3.04 (m, 2H, CH₂-ph), 2.41 (s, 3H, bpy-CH₃), 1.03 (t, J = 6.8 Hz, 3H, COOCH₂CH₃).

Ru(II)(4,4′-di-COOH-2,2′-bpy)₂(4-Me-2,2′-bpy-4′-CONH-l-alanine Ethyl Ester)(PF₆)₂ (1a). The procedure for the preparation of this compound was similar to that for **1**. ¹H NMR (400 MHz, D₂O), δ in ppm: 8.85 (s, 4H, 4,4′-di-COOH-bpy-H), 8.71 (s, 1H, 4′-Me-bpy-H), 8.38 (s, 1H, 4′-Me-bpy-H), 7.78−7.83 (m, 5H, 4,4′-di-COOH-bpy-H (4H) + 4′-Me-bpy-H (1H)), 7.60−7.66 (m, 4H, 4,4′-di-COOH-bpy-H), 7.55 (d, J = 5.6 Hz, 1H, 4′-Me-bpy-H), 7.46 (d, J = 5.6 Hz, 1H, 4′-Me-bpy-H), 7.17 (d, J = 5.6 Hz, 1H, 4′-Me-bpy-H), 4.45 (m, 1H, CH(COOEt)), 3.43 (q, J = 6.8 Hz, 2H, COOCH₂CH₃), 2.42 (s, 3H, bpy-CH₃), 1.41 (2, J = 7.2 Hz, 3H, CH(COOEt)CH₃), 1.05 (t, J = 6.8 Hz, 3H, COOCH₂CH₃).

Synthesis of Nanocrystalline Colloidal TiO₂. Nanocrystalline colloidal TiO₂ particles were prepared by a controlled hydrolysis of TiCl₄ as proposed by Kormann et al.[22] A 2 mL portion of TiCl₄ cooled to −20 °C was added slowly to 514 mL of vigorously stirred distilled water at 1 °C. After stirring for 30 min at this temperature, the reaction mixture was dialyzed for 1 h (Spectropor membrane) using 1 L of distilled water. The dialysis procedure was repeated 4 times to change the pH of the solution from 1 to 2.4. The dialysis also improved the stability of the colloid and facilitated the formation of TiO₂ crystals. Evaporating the solvent by a rotary evaporator at 30 °C and 25 mbar led to the formation of a white-yellowish crystal, which was dissolved in distilled water to obtain a perfectly transparent colloidal TiO₂ suspension. The quality of the obtained particles was tested by analyzing the UV−Vis absorption spectrum, according to the method suggested by Kormann et al.[22] The plot of the natural logarithm of the absorption coefficient against the photon energy yields the band gap energy (E_{gap}) of 3.4 eV, which is comparable to the value obtained by Kormann et al., E_{gap} = 3.2 eV, for an average particle diameter of 2.4 nm.

Spectroscopic Measurements. Luminescence spectra were recorded using a SPEX Flurolog fluorimeter by exciting the sample at 450 nm. Absorption spectra were recorded on a Jasco-V-530 spectrophotometer in a 1 cm quartz cell. Transient absorption experiments were conducted with a nanosecond laser flash photolysis setup. The excitation pulse at 450 nm was obtained from a Quanta-Ray master optical parametric oscillator (MOPO) pumped by a Quanta-Ray 230 Nd:YAG laser, having a pulse energy of 1−2 mJ and duration of ≈7 ns. The probe light from a xenon arc lamp (75 W) was focused to a 1 mm diameter spot overlapping with the unfocused pump beam of 2.5 mm diameter. After passing through the 1 cm quartz cell containing the sample, the probe light was passed through two single grating monochromators and detected by a photomultiplier tube Hamamatsu R928.

The stock solutions of **1** and **1a** were prepared in distilled water and stored in the dark. A transparent colloidal TiO₂ solution was prepared by dissolving the TiO₂ crystals in distilled water. The sample solution was prepared by adding a few microliters of TiO₂ solution to freshly prepared solutions of **1** or **1a** to obtain the desired concentration, and the pH value was measured with a standard pH meter.

Absorption spectra were measured before and after flash photolysis measurements to check whether photochemical changes occurred during the experiment. No sample degradation was observed during the flash photolysis experiment. The transient spectra at different delay times were constructed from average kinetic traces measured at different wavelengths. All kinetic traces and spectral profiles were fitted using data analysis package Microcal Origin.

Results and Discussion

Synthesis. The synthesis of complex **1** (Scheme 1) was started with the ligand 4-methyl-4′-carboxy-2,2′-bipyridine, **2**, which was prepared according to the modification of a literature method.[20] Conversion of the carboxylic acid into its acid chloride form was performed by refluxing **2** in thionyl chloride, followed by a reaction with l-tyrosine ethyl ester hydrochloride in acetonitrile solution in the presence of triethylamine as base. This led to the formation of crude product **3** in which the tyrosine is linked to the bpy ligand via an amide bond. The purification of compound **3** was made by column chromatography on silica gel. Then, **3** was subjected to the coordination reaction with ruthenium(II) (4,4′-di-COOEt-2,2′-bpy)₂Cl₂ (**6**), which was synthesized from 4,4′-di-COOEt-2,2′-bpy (**5**) by a modification of the literature procedure.[21] It was found that when methyl esters (4,4′-di-COOMe-2,2′-bpy) were used instead of **5**, the reaction gave a complicated mixture of complexes because of the instability of methyl esters in this special case. The complex with carboxyl groups is normally difficult to handle during a purification procedure. Therefore, purification was performed for its ester form, **7**, because it can be purified by normal column chromatography. No attempts of further purification with column chromatography were made after the hydrolysis of the esters in **7**, to give the final product **1**, which was characterized by NMR. Complex **1a** was synthesized by a similar route as for **1**, using l-alanine ethyl ester hydrochloride as the starting material instead of l-tyrosine ethyl ester hydrochloride (Scheme 1). Both

Scheme 1. Synthetic Routes for Complex **1** and **1a**
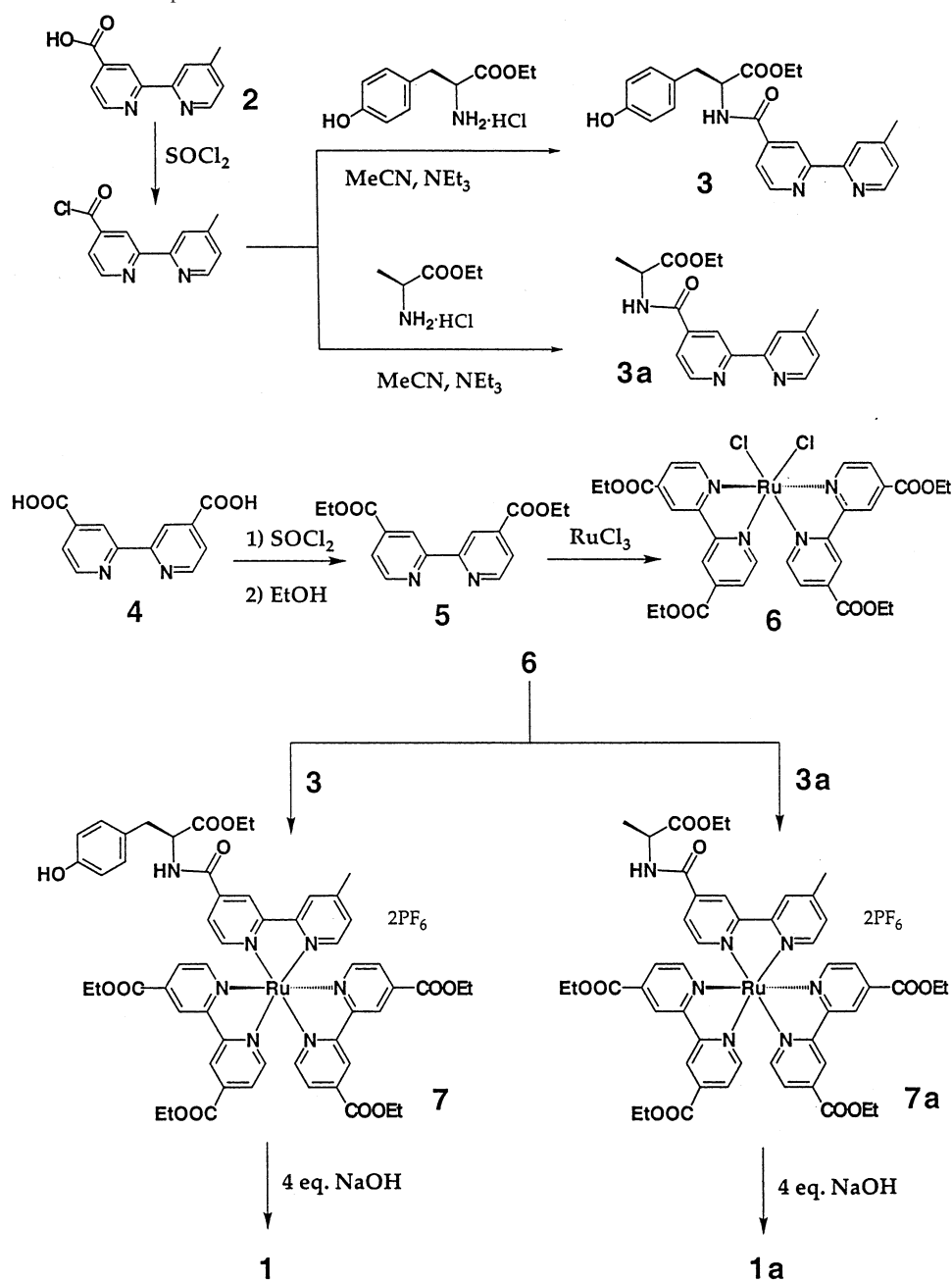
complexes **7** and **7a** were characterized by ^{1}H NMR and electrospray ionization mass spectrometry (ESI-MS).

Photophysical Properties. Figure 2 shows the absorption and emission spectra of **1** and **1a**. The absorption spectrum of **1** and **1a** exhibits the characteristic bands found in ruthenium complexes[5] such as Ru(bpy)$_3^{+2}$, where the intense ligand-centered band (LC) at 301 nm arises from a π to π^* transition and the band at 475 nm is assigned to a metal-to-ligand charge transfer (MLCT) as a result of a d to π^* transition.

For both complexes **1** and **1a**, the MLCT band at 475 nm is red-shifted by 25 nm compared to the typical MLCT band in the analogue Ru(bpy)$_3^{+2}$ (λ_{max} at 450 nm). This red shift of the MLCT band occurs because of the presence of the carboxylic acid groups; the withdrawing nature of the carboxylic acid groups lowers the energy of the π^* orbital

of the ligand, causing the d to π^* transition to occur at lower energy.[11] On the other hand, deprotonation of the carboxylic acid group affects the LUMO energy of the ligand in such a way that the MLCT band is blue shifted to higher energy by 10 nm from 475 to 465 nm upon increasing the pH of the solution from 1 to 7.[19] The lowest MLCT excited state exhibits an intense luminescence emission band at 650 nm at pH 1, and it is also blue shifted by 25 nm, from 650 to 625 nm, at pH 7.

Favorable conditions for adsorption of the dye molecules to the TiO$_2$ surface could be achieved if conditions of electrostatic attraction between the TiO$_2$ and sensitizer were established. For the sensitizer, the pK_a value reveals its electrostatics properties. The shift of the MLCT absorption band at 470 nm of **1** as a function of pH was used to determine the pK_a value of the ground state.[13] A plot of the
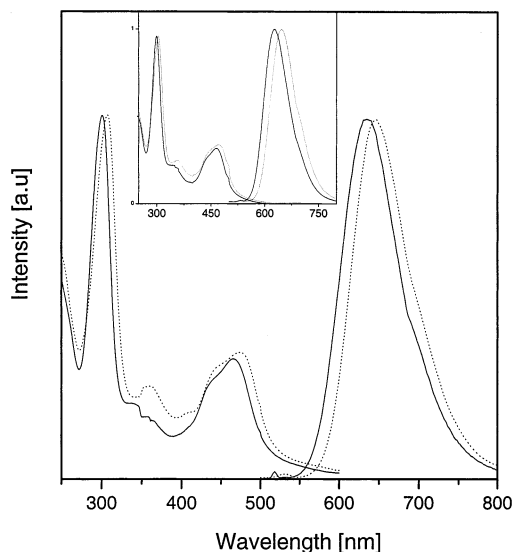
Figure 2. Normalized absorption and emission spectra of complexes **1** and **1a** (inset) recorded at pH 7 (—) and pH 1 (···). The emission spectra were excited at 450 nm.

Figure 3. Luminescence emission spectra of **1** in the presence of various concentrations of TiO₂, [**1**] = 15 μM. Excitation at 450 nm.

λ(max) of the MLCT transition as a function of pH shows a sigmoidal shape (data not shown), with a pH at the inflection point giving the ground state value of 2.0 ± 0.1 and another at pH $= 0.4 \pm 0.2$. These values are assigned to the pK_{a1} and pK_{a2} of the carboxylic acid groups. It is known that TiO₂ has an isoelectric point at pH $= 5$;[23] that is, below a pH of 5 the TiO₂ is positively charged [TiOH⁺], and at pH > 5 it is negatively charged. Thus, at pH < 5 we have the desired situation of negatively charged dye and positively charged TiO₂ surface, providing favorable electrostatic attraction for adsorption of complexes **1** and **1a** to the semiconductor surface. However, taking into account also the stability of the TiO₂ colloid[14] and agglomeration[15] due to the accumulation of charge at low pH, the condition of strong electrostatic interaction between the dye and TiO₂ is maintained up to pH ≈ 4. Attachment of complex **1** or **1a** to the TiO₂ surface in this pH interval was examined by observing the quenching of luminescence by the TiO₂. As shown in Figure 3, the luminescence intensity of **1** is decreased with the increase of the TiO₂ concentration until it reaches a constant value at concentrations of about 120 μM. The dye adsorption to TiO₂ also causes a small increase of the overall absorbance of **1** and a small red shift from 466 to 473 nm. These spectral changes are due to the changes of the acidity upon increasing the TiO₂ concentration. A corresponding shift of the emission maximum ($\sim$25 nm) is also observed at high TiO₂ concentration. The similarity of the quenching pattern observed for both complexes shows that the presence of the tyrosine in **1** does not affect the functionality of the carboxylic acid group, which makes the following analysis valid for both complexes **1** and **1a**.

The observed quenching of the MLCT excited state was shown to be due to an electron transfer to the semiconductor.[14,16,23] The quenching behavior observed here is similar to the quenching by TiO₂ observed for other ruthenium
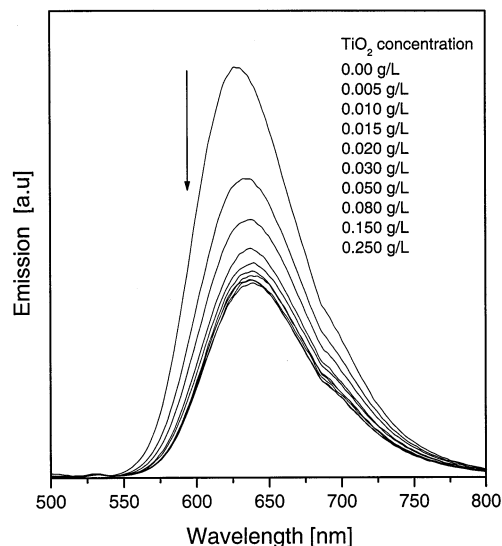
dyes[17,18] as well as for fluorescein,[10] anthracene,[16] and eosin[23] and is attributed to electron injection from the excited state of the dye to the conduction band of TiO₂.[12] This process is thermodynamically allowed because the excited state energy of complex **1** is at -3.34 eV and the low energy edge of the conduction band of TiO₂ is below, at approximately -4.2 eV. According to Kamat et al.,[16,24] the quenching of luminescence by the TiO₂ colloidal particle reflects the amount of chemisorbed dye on the surface of the TiO₂ particle. To obtain an association constant (K_a) for the dye−TiO₂ interaction, quenching of the luminescence intensity of **1** and **1a** by TiO₂ was analyzed by considering an equilibrium between the adsorbed and unadsorbed dye molecules.

$$\text{dye−COO}^- + \text{TiOH}^+ \underset{}{\overset{K_a}{\rightleftharpoons}} [\text{dye−COO−Ti}\equiv] \quad (1)$$
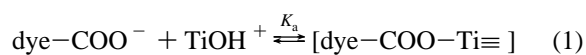
The observed emission quantum yield ϕ_f of the dye in the presence of colloid is related to the emission quantum yield of the unadsorbed dye, ϕ^o_f, and the emission quantum yield of adsorbed molecule, ϕ'_f, by the following eq 2

$$\phi_f = (1 - \alpha)\phi^o_f + \alpha\phi'_f \quad (2)$$

where α is the degree of association between the TiO₂ particles and **1**. Under the condition of high TiO₂ concentration ([TiO₂] $\gg$ [dye]), α can be expressed as

$$\alpha = \frac{K_a[\text{TiO}_2]}{1 + K_a[\text{TiO}_2]} \quad (3)$$

By substituting eq 3 into eq 2, the quenching of luminescence emission of **1** or **1a** by TiO₂ can be represented as

$$\frac{1}{(\phi_f^\circ - \phi_f)} = \frac{1}{(\phi_f^\circ - \phi'_f)} + \frac{1}{K_a(\phi_f^\circ - \phi'_f)[\text{TiO}_2]} \quad (4)$$

(23) Moser, J.; Grätzel, M. *J. Am. Chem. Soc.* **1984**, *106*, 6557.

(24) (a) Xiang, J.; Chen, C.; Zhou, B.; Xu, G. *Chem. Phys. Lett.* **1999**, *315*, 371. (b) Kamat, P. *Chem. Rev.* **1993**, *93*, 267.

The emission quantum yields (ϕ) were measured by comparison of the emission spectrum of the sample with the emission spectrum of a reference compound (tryptophan) using the following equation:

$$\phi_x = \frac{D_x}{D_r} \frac{A_r(\lambda_r)}{A_x(\lambda_x)} \phi_r \tag{5}$$

where D is the area under the luminescence spectrum, $A(\lambda)$ is the corresponding absorbance at the excitation wavelength, and the subscripts r and x refer to reference and sample solutions.[25] The experimental data were fitted using eq 4, and an apparent association constant K_a of 4.1×10^4 M^{-1} as well as the emission quantum yield of the adsorbed molecule ($\phi_f' = 0.005$) were obtained. The same quenching pattern was observed for reference compound **1a**, with a similar association constant as for **1**. This shows that under our experimental conditions approximately 80% of complex **1** or **1a** is adsorbed to the surface of TiO$_2$.

Photoinduced Electron Transfer. Aqueous solutions containing 15 μM of **1** or **1a** and 120 μM of TiO$_2$ at pH = 2.4 were used for the flash photolysis measurements. The electron transfer processes were initiated when a pulse of visible light (λ = 450 nm) was used to excite the MLCT band of Ru(II) and promote an electron from a Ru d orbital to a π^* orbital of the ligand, from which an electron can be injected into the conduction band of TiO$_2$. As a result, the dye cation Ru(III) is formed, and the Ru(II) MLCT ground state absorption is bleached. From several studies,[10,17,18,24] it is known that, when a dye is adsorbed on the surface of a nanocrystalline TiO$_2$ semiconductor, the rate and yield of electron injection into TiO$_2$ depend on the relative energies of the semiconductor conduction band edge and the excited state of the dye. For favorable energetics of injection, ultrafast subpicoseconds to picosecond electron transfer from the dye to semiconductor have been reported for a number of different systems.[10,17,18] Thus, we conclude that the electron injection from **1** and **1a** into TiO$_2$ occurs analogously to that of other ruthenium dyes,[17–19] implying that the electron injection is indeed much faster than the diffusion controlled electron transfer recorded in the presence of an external electron acceptor.[8] Hence, for complex **1** attached to the nanocrystalline TiO$_2$, the second electron transfer from the tyrosine moiety to the dye cation Ru(III) is the rate-limiting step. Once the dye cation Ru(III) is formed, there are in principle two possible ways for the photogenerated Ru(III) to return to the Ru(II) ground state: either by back electron transfer from the nanocrystalline TiO$_2$ (charge recombination) or by a second intramolecular electron transfer process from the linked tyrosine moiety.[6,8] Both reactions will result in repopulation of the Ru(II) ground state and thus recovery of the Ru(II) ground state bleaching. To distinguish between these pathways, other spectral features of the transient absorption spectra must be investigated.

The temporal evolution of the transient absorption spectra of the **1**−TiO$_2$ system, Figure 4A, shows that the absorption
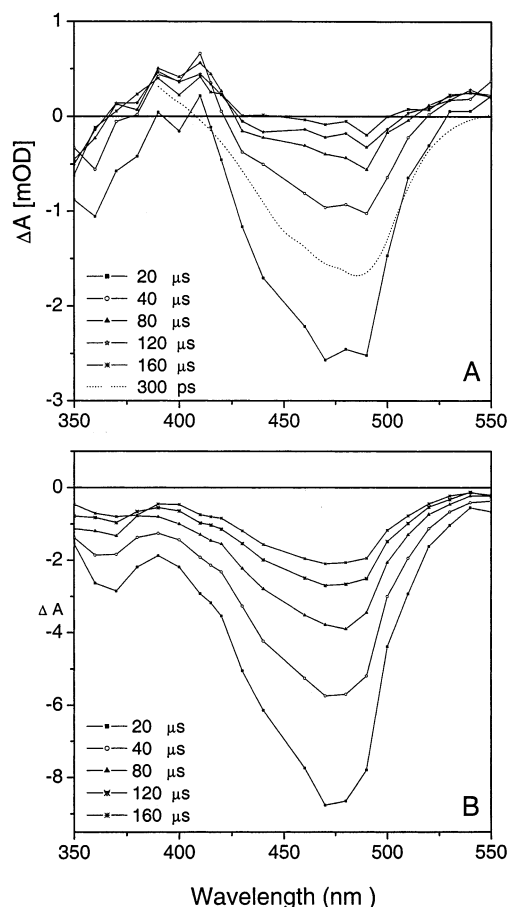

Figure 4. Transient absorption spectra of adsorbed complexes **1** (A) and **1a** (B) at pH 2.4 and 15 μM for both complexes **1** and **1a** with 120 μM TiO$_2$ at different delay times after excitation at 450 nm. In panel A, the transient absorption spectrum recorded at 300 ps was normalized to allow a direct comparison with the spectra recorded at microsecond delays.

recovery of Ru(II) is accompanied by the appearance of a new spectral feature located at 410 nm. This positive band can be attributed to the formation of the tyrosyl radical, which is known to exhibit an absorption band at 410 nm.[26]

Generally, a positive signal in transient absorption spectra may originate from the absorption of excited states or any product generated from the excited state. Thus, it is possible that the 410 nm band originates from the absorption band of photogenerated Ru(III) or from excited states of Ru(II). To exclude this possibility, we have measured the transient absorption at 300 ps after excitation.[27] At this delay, the Ru-(III) is certainly formed because the electron injection occurs on the subpicosecond to picosecond time scale. It is clear from Figure 4A that the 300 ps transient spectrum does not exhibit a distinct spectral band around 410 nm, which excludes the possibility that the 410 nm absorption band originates from the absorption of the Ru(III) formed by electron injection. This provides additional support for an assignment of the 410 nm band to the tyrosyl radical, indicating the tyrosyl radical is indeed formed as a result of

(25) Szabo, A, G.; Rayner, D. M. *J. Am. Chem. Soc.* **1980**, *102*, 554.

(26) Land, E. J.; Prutz, A. *Int. J. Radiat. Bio.* **1979**, *36*, 75.
(27) Measurements with picosecond time resolution were conducted with a different experiment setup; for description of the system, see refs 10 and 18.

the intramolecular electron transfer from the tyrosine moiety to the photogenerated Ru(III).

A definite assignment of the absorption band at 410 nm to the tyrosyl radical proving the presence of intramolecular electron transfer from the linked tyrosine moiety to the photogenerated Ru(III) was achieved in a separate experiment on the analogue complex **1a** which lacks the tyrosine moiety. Thus, no absorbance feature due to the generation of a tyrosyl radical should be observed for this molecule. Figure 4B shows the transient absorption spectra of the reference complex **1a** attached to nanocrystalline TiO₂ measured under identical experimental conditions as those used for **1**. As in case of **1**−TiO₂, after exposing the **1a**−TiO₂ solution to a laser flash, strong bleaching of the MLCT band was observed as a result of electron injection into TiO₂, followed by absorption recovery at 470 nm. A direct comparison of the transient absorption spectra and kinetics of both complexes reveals two important points. First, the absorption recovery of reference complex **1a** is apparently slower than the absorption recovery recorded for **1**. Also, while the bleaching signal is almost gone after 100 μs in the case of complex **1**, bleaching signal for complex **1a** did not recover to the baseline within this time. Second, the positive band at 410 nm is absent in the transient absorption spectra of **1a**. This is clear proof that the tyrosine moiety is responsible for the appearance of the positive band at 410 nm. In other words, the tyrosyl radical is formed as a result of intramolecular electron transfer from the tyrosine part of **1** to the photogenerated Ru(III), while, for reference complex **1a**, which lacks the tyrosine part, this step no longer exists. To ensure that the observed electron transfer is indeed intramolecular, the kinetics were measured for a few concentrations of **1** and **1a**, and no concentration dependence was found confirming our assignment of intramolecular electron transfer. The absorption recovery of Ru(II) absorption that is still observed in **1a** occurs as a result of recombination between electrons in nanocrystalline TiO₂ and Ru(III). Taking into account the absorption coefficients of the tyrosyl radical ($\epsilon = 3000$ M⁻¹ cm⁻¹) and **1** ($\epsilon = 15000$ M⁻¹ cm⁻¹), the yield of Ru(III) to tyrosyl radical conversion can be estimated from the relative absorption magnitude of Ru(II) ground state bleaching at early times (~0.5 μs) and the 410 nm band corresponding to the tyrosyl radical. This estimation gives a tyrosine−ruthenium electron transfer yield of about 15%. As shown later, this low yield of tyrosine−Ru(III) electron transfer is explained by a fast back electron recombination process from TiO₂ to Ru(III). Comparison of the kinetics of Ru(II) absorption recovery at 470 nm for **1** and **1a** (Figure 5A) shows that it is faster for complex **1**. On the other hand, the absorption recovery of complex **1a** reflects the dynamics of the back electron recombination between TiO₂ and Ru(III) as it is the only pathway for the recovery of the originally excited Ru(II). Thus, a direct comparison of the kinetics shown in Figure 5A enables us to obtain the time constants of tyrosine−Ru(III) electron transfer and the back electron transfer recombination.

A multiexponential fit of the 470 nm kinetics of **1a** (Figure 5A) results in the time constants $\tau_1 \approx 0.5$ (73%) μs, $\tau_2 =$
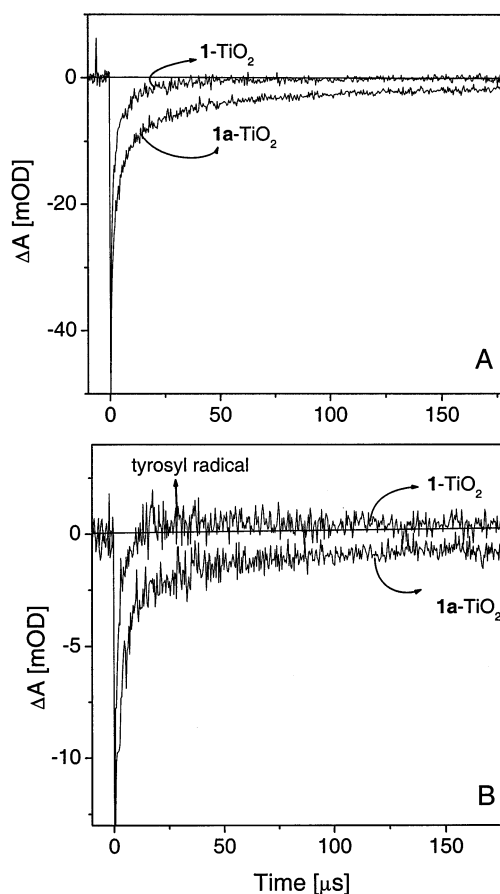

Figure 5. Kinetics of adsorbed complexes **1** and **1a** measured after 450 nm excitation at pH 2.4 and 15 μM concentration for both complexes **1** and **1a** with 120 μM of TiO₂. Kinetics were recorded at 470 nm (A) and at 410 nm (B).

4.4 ± 0.3 (13%) μs, and $\tau_3 = 20 \pm 3$ (14%) μs. The fastest ≈0.5 μs component is partly due to the unadsorbed dye molecules having a lifetime of 0.72 μs. In addition, it is known from other studies that the charge recombination is a highly multiexponential process and that a part of the recombination can occur also on nanosecond time scales. Thus, a part of the ≈0.5 μs component is also due to the fast charge recombination. The two longer time constants reflect the recombination between Ru(III) and electrons injected into TiO₂, corresponding to an effective average rate constant of 3.2×10^5 s⁻¹, in accord with other reports.[17,19] Fitting of the 470 nm kinetics for complex **1**, which necessarily contain also a component corresponding to the tyrosine−Ru(III) electron transfer, yields in fact almost the same time constants as for complex **1a**. The amplitudes of the kinetic components are, however, different: $\tau_1 = 0.5$ (73%) μs, $\tau_2 = 4.2 \pm 0.3$ (20%) μs, $\tau_3 = 20$ (7%) ± 3 μs, resulting in an effective average rate constant of 4.4×10^5 s⁻¹ for the combined tyrosine-to-Ru(III) and TiO₂-to-Ru-(III) electron transfer process. For complex **1**, kinetics measured at 410 nm (Figure 5B) correspond to the formation of the tyrosyl radical, and the same time constants as at 470 nm are obtained. For complex **1a**, which has no tyrosine moiety, kinetics measured at 410 nm naturally reflect only absorption recovery due to the recombination between Ru-(III) and TiO₂ electrons. That rate constant for the intramo-

lecular electron transfer from tyrosine to Ru(III) found here is faster than the one obtained for a comparable complex in the presence of an external electron acceptor MV^{2+} in solution.[8] It is obvious that the use of TiO_2 as an electron acceptor suffers from competitive back electron recombination occurring on a similar time scale as tyrosine−Ru(III) electron transfer. The similarity of these time scales does not allow us to clearly separate these two processes and also accounts for the low yield of the tyrosine−Ru(III) electron transfer.

Conclusion

Synthesis and characterization of new Ru(bpy)$_3$ complex **1** with four carboxylic acid groups linked to the bpy ligands is described. The presence of the four carboxylic acid groups enables anchoring of the complex to nanocrystalline TiO_2 with a good degree of association (up to 80%). Attachment of the dye complex to the nanocrystalline TiO_2 enables ultrafast injection of electrons from the excited MLCT state into the conduction band of TiO_2. This simplifies the study of the second intramolecular electron transfer from the tyrosine moiety to the photogenerated Ru(III) because this step is now rate limiting. The intramolecular electron transfer from the tyrosine moiety to the Ru(III) led to the formation of the tyrosyl radical which can be observed at 410 nm. The yield of Ru(III)−tyrosyl radical conversion was limited to ≈15%, as a result of fast competing charge recombination between Ru(III) and photoinjected electrons in the TiO_2. It appears necessary for the design of a more efficient complex to construct a molecule with the positive charge density of the cation state located on Ru away from TiO_2, favoring a slow charge recombination and enhancement the Ru(III)-to-tyrosyl radical conversion.